The role of influenza neuraminidase transmembrane domain on budding and virus morphology

Scott E.Roddy

Supervisor: Dr. Jeremy S. Rossman

Ingram 238

The University of Kent

8th of August 2014

Abstract

Influenza A virus neuraminidase (NA), a type II transmembrane glycoprotein plays a role in the cleavage of sialic acids and facilitating the release of mature virions from the surface of infected cells. NA has also previously been shown to play a role in virion formation during influenza A virus budding, although the exact mechanisms by which NA contributes to influenza virion formation and morphology is currently unknown. Previous research has shown that mutations within the transmembrane domain (TMD) of NA can result in alteration in virion morphology, particularly in the production of filament like influenza virions. In this research project we examined if the TMD does indeed play a role in influenza virus budding and morphology. We utilised both full and partial mutations of the TMD of NA from A/WSN/33, a primarily spherical lab adapted influenza strain, with the TMD of a primarily filamentous strain A/California/09. To evaluate the effects of TMD on the morphology of a primarily spherical strain with that of filamentous strain. This study used a transfection based virus like particle (VLP) system to examine the effects of TMD alterations on morphology, utilising various biochemical and microscopy methods. Our findings show that as previously indicated mutations within the TMD do result in alterations to virion morphology, as well as showing that despite previous theories both NA and NA's TMD may play a more active role in in budding and morphology than previously thought.

Abbreviations

HEK 293T cells – Cambridge Human embryonic Kidney 293 T cells

AMP – Ampicillin

CaCL – Calcium Chloride

Dmem + 10% FBS – Dulbeccos modified eagles medium with 10% Fetal bovine serum

E. coli – Escherichia Coli

HA – Hemagglutinin

HindIII – Restriction enzyme cutting pCAGGS plasmid at 2275 base pairs

Kan – Kanamycin

LB – Lysogeny Broth

M1 – Influenza matrix protein 1

M2 – Influenza matrix protein 2

NA – Neuraminidase

NP – Nucleoprotein

NS1–Non structural protein 1

NS2–Non structural protein 2

PA– Influenza viral polymerase molecule

PB1– Influenza viral polymerase molecule

PB2– Influenza viral polymerase molecule

PBS– Phosphate buffered saline

Pen– Penicillin

RNA– Ribonucleic acid

RNP– Ribonucleoprotein

SDS Page– Sodium dodecyl sulphate polyacylamide gel electrophoresis

SOC– super optimal broth with catabolite repression

Strep– Streptomycin

TEM– Transmission electron microscopy

VLP– Virus like particle(s)

XhoI– Type 2 restriction enzyme that cuts pCAGGS plasmid at 1725 base pairs

Contents

Introduction

The influenza virus is a member of the viral family orthomyxoviridae, both pandemic and seasonal variations of the virus are responsible for worldwide outbreaks of respiratory and gastrointestinal illness. Seasonal flu accounts for around 250,000 to 500,000[1] deaths alone, with those most at risk being the young, old and immune compromised, due to complications such as secondary infections. Continuous evolution and mutation of the influenza virus leads to the production of seasonal and pandemic strains of the influenza virus. The classification of influenza virus is dictated by the type of hemagglutinin (HA) and neuraminidase (NA) surface glycoprotein expressed on the surface of the mature virus. It is these two surface glycoproteins HA and NA which are recognised by the immune system and responsible for a person's immunity to the varying strains of the influenza virus.

Seasonal strains of the virus are the result of "antigenic drift"[2]. Antigenic drift is due to a number of minor mutations within HA and NA, resulting in the production of a virus that is similar in phenotype to its predecessor, but due to minor mutations in HA and NA has a different antigenic profile. This difference in antigenic profile means that on average within a given population there will be low previous immunity to the virus. It is this process of antigenic drift which requires the continuous surveillance of influenza strains within a population, and the updating and production of a new influenza vaccine yearly.

Pandemic strains are the result of a process known as "antigenic shift"[3], where up to three different strains of the influenza virus infect the same host. During replication there is a genetic mixing of segmented viral genome leading to the production of new virus, which has a novel combination of HA and NA surface proteins not seen in the current repertoire of influenza viruses within the host population. Typically the novel composition of the surface glycoproteins of the pandemic strain will differ widely from the seasonal strains within the

current population, this results in the production of a strain where there is no previous immunity to the virus within the population, and where immunisation strategies at the time of emergence are ineffective at providing any immunity or protection from the virus. Leading to the rapid spread of the virus and high mortality within those infected, the best know historical example of this is the 1918 H1N1 "Spanish flu" pandemic that spanned the globe and resulted in 50 million deaths over a two year period[4].

The influenza virus is a member of the viral family orthomyxoviridae made up of three different categories of influenza viruses, A, B and C all of which cause pathogenesis in humans[1]. The typical structure of influenza virus is a filamentous or spherical virion. The typical anatomy of an influenza virion (Figure 1) is a lipid capsule surrounding the capsid and RNA nucleoprotein core of the virus. The viral glycoprotein's hemagglutinin (HA) and neuraminidase (NA) span the outer lipid membrane of the mature influenza virion, and are involved in initiating virus entry into a host cell[5,6]. Matrix protein 1 (M1) forming a second layer of the virion connecting the outer lipid bilayer and ribonucleoprotein core[7] (RNP). Matrix protein 2 (M2) is a proton selective ion channel, and is involved in balancing the pH across viral membrane during entry into the host cell and viral replication[8,9]. The ribonucleoprotein core consists of the viral nucleoprotein (NP) that is involved in packing the viral genome during budding and replication, as well as RNA polymerase complex proteins PA, PB1 and PB2[10,11]. Other proteins are involved in process of replication but are not found in the mature virion such as non-structural protein 1 (NS1)[12] involved in evasion of the host immune system , non-structural protein 2 (NS2)[13] or nuclear export protein involved in exportation of the viral proteins form host cell's nucleus. And PB1-F2[11] which is involved in causing apoptosis of the virally infected cell, although PB1-F2 is not found in all strains of the influenza virus. Eight of these proteins are produced and packaged into virion upon replication[14].

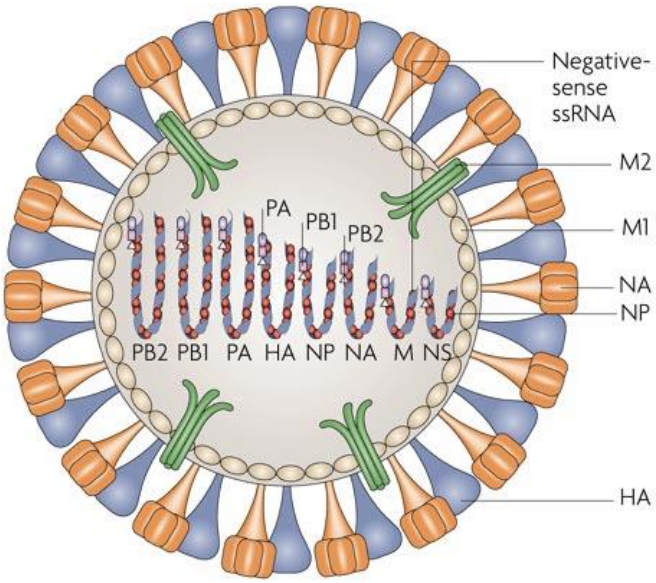

Fig1: Cartoon depicting the typical structure of a mature spherical influenza virion adapted from [37]. Showing two surface glycoproteins hemagglutinin (HA) in blue and neuraminidase (NA) in orange. Matrix protein 1(M1) and matrix protein 2 (M2) in green. And a depiction of segmented viral genome and ribonucleoprotein core.

Viral budding and virion morphology

The process of budding is where a mature influenza virion is assembled and released form an infected cell. Based on recent research, the currently proposed model of budding[14] is thought to be initiated by glycoproteins HA and NA being transported and expressed on the surface of infected cell. HA and to a lesser extent NA are thought to cause recruitment and concentration of lipids raft domains in the cell membrane into high concentration lipid raft domains called the viral budozone[15 5]. This clustering of lipid raft domains is thought to initiate membrane curvature and recruit M1 to newly budding virion. M1 then polymerases through binding to cytoplasmic tails (CT) of HA and NA, this polymerisation results in further membrane curvature and formation of budding immature virion. The polymerisation of M1 is thought to act as a binding site for RNP and NP, which in inhibits M1's ability to alter membrane curvature. The Binding of M1 is thought to also recruit M2 to low lipid area at

the base of budding virion between virion and cell membrane, caused through the depletion of high lipid raft domains through the concentration of these areas by HA and NA. This depletion of lipid raft domains allows M2 to insert its amphipathic helix into cell membrane, causing tension change between lipid phase and resulting in lipid packing defects within the membrane, resulting in positive membrane curvature [16]. This positive membrane curvature is thought to be powerful enough to allow the pinching, membrane scission and release of mature virion from the infected cell.

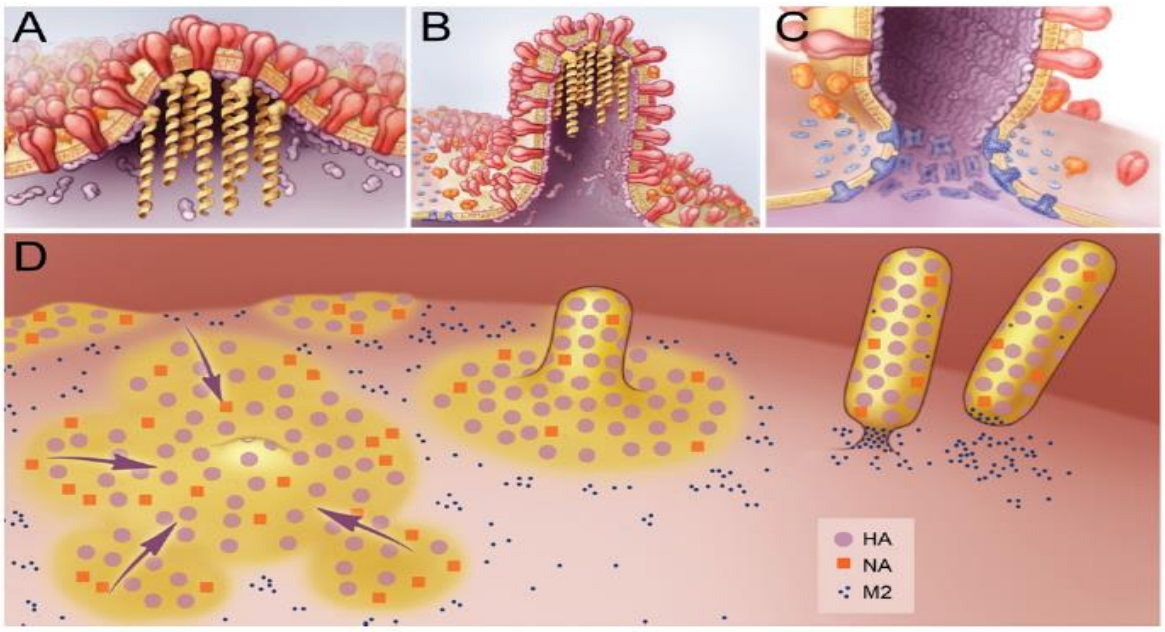

Fig 2: Proposed model of budding and release of mature influenza virion Adapted from Rossman et al 2011 [14]. Section (A) demonstrating HA (Red) and NA (Orange) causing the clustering of lipid raft domains into viral budozone, causing membrane curvature and initiation of budding. (B) showing the continuation of budding through recruitment and binding of M1 (purple) to the CT of HA and NA. Polymerisation of M1 causing the recruitment of RNP core and viral genome into the budding virion. (C) Demonstrating the recruitment of M2 (Blue) by M1 into the low cholesterol area at the base of budding virion known as the neck. Where M2 inserts its amphipathic helix resulting in positive membrane curvature and membrane scission resulting in the pinching off and release of mature virion from the infected cell. (D) Showing the overall process of budding from coalescence of lipid rafts through to release of budding virion.

Mature influenza virions can exist in two distinct morphologies, either a round spherical virion or long filamentous virion. Spherical virions typically measure 100 nanometers (nm) in

size and are found mainly in primary isolates, lab adapted strain and in some clinical samples. Mature filamentous virions are typically pleomorphic in shape, measuring up to 30 µm in length and 100nm in diameter. Filamentous virions are typically found in samples taken from clinical isolates. Despite varying differences in size and morphology of two virions previous research has found that filamentous virions possess similar expression of viral proteins and no observable differences in the structure of viral genome compared to spherical virions [17].

The reason for these two distinct morphologies along with the exact mechanisms behind budding, the exact mechanism that control or select for the expression of filamentous or spherical virions are not yet fully understood. It was previously theorised that filamentous or spherical morphology may aid in the transmissibility of virion or confer some survivability traits which may help the virion survive outside host or infect another host. Numerous studies have found very little significant difference between the transmissibility or infectiousness of different virion morphologies[18]. Another theory is that spherical or filament formation may be a result of adaption to a growth in a specific host. As it has been repeatedly observed since the 1960's that repeated passaging of a primarily filamentous isolates in eggs result in the loss of filamentous morphology [19 20].

As mentioned above the exact mechanisms behind filament formation are currently unknown, but there has been a large amount of research into discovering the exact mechanisms budding with viral proteins M1 [21,22], HA,NA[23 5 13 24] and M2 [21 25] being thought to be responsible for filament formation.

Neuraminidase and its role in virus morphology

NA is a tetramic type II membrane glycoprotein, responsible for the enzymatic cleavage of sialic acid residues promoting release of newly formed virion from surface of infected cell and preventing the aggregation of virions during budding and release of budding virions[26].

The basic structure of NA consists of four distinct parts, enzymatic head domain which gives NA its characteristic mushroom like structure, responsible for its enzymatic activity. Variable stalk, thought to regulate the height of head domain in accordance to cell surface receptor height which along with the head region makes up the ectodomain. Also containing the transmembrane domain (TMD) anchoring NA to viral membrane and highly conserved cytoplasmic tail (CT) [6].

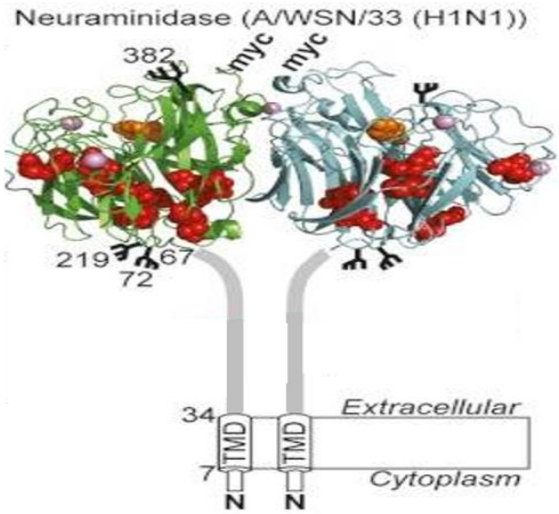

Fig 3: Typical structure of Influenza A type II transmembrane glycoprotein neuraminidase (NA) shows stereotypical "mushroom" like shape. Consisting of the ectodomain made up of enzymatic head domain responsible for cleavage of sialic acid, and the variable stalk region. Adapted from Da silva et al 2013 [30]

NA has on numerous occasions been shown to play a more direct role in budding than previously thought. With studies and previous work in our laboratory [5] [27] showing that in plasmid based virus like particle systems (VLP) NA is not only able to induce membrane curvature and produce virus like particles from transfected cells. But is also able to facilitate the release of these virus like particles from the surface of transfected cells. And that NA is also seemingly capable of producing both spherical and filamentous VLP's in these plasmid based system, conferring that NA may play a more direct role than previously thought.

In terms of exact mechanism of NA's role in budding and virus morphology a large volume of previous studies have been directed towards the enzymatic head domain of NA, due to the conserved nature of TMD and CT amino acid sequences amongst differing strains and morphologies, the latter being highly conserved. Because of this the TMD has been relatively understudied.

Transmembrane domain role in NA structure and function

Despite the lack of study several studies that have been done to explore the role of TMD both towards NA's involvement in budding and towards the assembly and structural properties that TMD confers within NA have shown several key findings.

Research [28] [29] has shown that TMD can play a role in virus morphology. In the referenced studies it was found that when various mutations within the TMD of influenza A virus strain A/WSN/33 a classically spherical strain were made, that these mutations resulted in significant alterations in virus morphology upon infection of Madin- Δarby canine kidney cells (MDCK). These findings suggest that the TMD may play a direct role in virus morphology or may affect the assembly of NA in a way that alters virus morphology.

Very recent studies [30,31] have shown that the TMD may play a more predominant role than previously thought. This study found when NA was expressed without its TMD NA was synthesised and transported to the plasma membrane correctly, but resulted in an inactive form of NA. Inactive NA was able to be rescued through the truncation of variable stalk region of inactive NA indicating that the TMD contributes and is required for NA maturation by effectively tethering the stalk to membrane allowing NA head domain to further drive assembly[31].

The study also found that varying polar residues and faces found within the TMD directly affect seemingly dictate the assembly of TMD from a dimer to a tetramer. With the study highlighting two distinct polar faces A and E faces of TMD that were found to be expressed adjacently across the NA subgroups N1, N3-N9 (S1), with the exception of N2 that was found not to have these widely conserved adjacent polar faces. And that these differences in localisation and interactions of various polar faces lead to differences in both the strength of interaction between TMD assembly and varying hydrophobicity of TMD, which is thought to result in alterations in TMD insertion and interaction with the plasma membrane (S1,S2). Indicating that the TMD may drive assembly along with enzymatic head domain through its anchorage of stalk region during insertion and formation of NA, along with alterations within the structure of the TMD may cause differing strength of interactions between NA and plasma membrane.

Based on these recent findings this research project aimed to explore the potential effect that the TMD and variation within the assembly of TMD have on the ability of NA to facilitate budding and its effect of virus morphology. As well as trying to further elucidate the role of NA in the process of influenza virus budding and potential interactions that take

place. Utilising a plasmid based virus like particle system along with other various biochemical and microscopy methodologies to fulfil these aims.

Methods

Cells

HEK 293T cells were maintained in Dulbecco's modified eagles medium (DMEM) (Sigma) supplemented with 10% fetal bovine serum (FBS) (Sigma), also containing 100 units/ml penicillin (Pen) and streptomycin (Strep). In a humidified incubator (Thermofisher) at 37 degrees and 5 % CO_2.

Plasmids

Both sets of plasmids pcDNA1.3 and NA76 Delta G 1.3 pcDNA3.1A sets of NA plasmids were kindly produced by Robert Daniels (University of Stockholm). Created through polymerase chain reaction (PCR) overlap cloning of pcDNA3.1A plasmid (Invitrogen) attached to a C terminal Myc-His Tag. Containing full length NA from H1N1 strain A/WSN/33.

Competent cells

A single colony of Top 10 *Escherichia Coli* (Invitrogen) were inoculated into lysogeny broth (LB) liquid medium and shaken at 37 degrees for 12 hours. 1ml of incubated culture was then in 100ml of LB medium and shaken at 37 degrees for 2 hours or until it reached an OD of 0.25 -0.3 at an OD_{600}. Culture was then chilled on ice and centrifuged for 10 minutes at 3300 g at $4^{\cdot C}$, supernatant discarded and resuspended in 40ml of 0.1M CaCL and placed in ice for 30 minutes. Cells were then centrifuged again at 3300 g at $4^{\cdot C}$ for 10 minutes and resuspended in 6ml of 0.1M CaCL and 15% glycerol solution (filter sterilised). 0.2ml of culture frozen at -70 degrees for a maximum of two months.

Recovery, transformation and extraction of plasmid stocks

Plasmid stocks recovered from filter paper via being soaked in 25µl of tris-EDTA (TE) buffer (Qiagen) and spun at max speed in a table top centrifuge (Thermo fisher) for 5 minutes. After which both sets of described plasmids were transformed using a heat shock

transformation method. Frozen competent cells thawed at room temperature for 10 minutes, with 10µl of suspended plasmid + TE buffer solution being added to 50µl of competent cells. Cells incubated on ice for 30 minutes, after which cells heat shocked at 42 degrees in a drybath (Thermo fisher) for 2 minutes. Placed on ice for a further 5 minutes before 60µl culture being placed in 940µl of LB, incubated at 37 degrees and 200 revolutions per minute(rpm) for 1 hour in a shaking incubator. Inoculated media then diluted 100 fold and 100µl plated on LB+Amp plates incubated at 37 degrees for 16 hours.

After transformation transformed cells scaled up through inoculation of 1 colony in 5ml of LB+Amp and incubated at 37 degrees and 200 rpm for 8 hours in a shaking incubator. 100µl of inoculated culture placed in 150ml of LB+Amp and incubated at 37 degrees and 200 rpm for 16 hours or until an optical density of 0.600 at 600 nanometers^{-1}(nm). Plasmids purified and recovered through Gen elute HP plasmid maxiprep kit (Sigma) as per manufactures instructions. Plasmid yield ascertained through nano drop spectrophotometer (thermo fisher) as per manufacture protocol.

Purified plasmids were checked for NA through a restriction digest on 1% agarose gel run at 90v and 180 amps using 1KB DNA ladder (Invitrogen) and 5x standard sample buffer in a novex gel tank (Invitrogen).

Analysis of VLP morphology

HEK 293T cells were seeded in 6 well dishes containing coverslips. Coverslips soaked in Poly-L-Lysine (Thermofisher) for 3 hours and rinsed 4 times before use. Cells were grown in 2ml DMEM-10%FBS +Pen/Strep for 16 hours at 37 degrees and 5% CO_2 until 60 % confluent. Cells were transfected using TransIT – 293 transfection reagent (Mirus) according to manufactures protocol, with 5µg of desired plasmid.

Cells incubated for 48 hours post transfection at 37 degrees and 5% CO_2, culture medium removed and transfected coverslips placed in 2ml of 10%formalin-Phosphate buffered saline (PBS) for 10 minutes. Coverslips were rinsed in 2ml PBS twice and edges aspirate, after which 200µl of blocking solution (DMEM + FBS) added to surface of each coverslip and incubated for 20 minutes. 200µl of primary antibody Myc tag mouse monoclonal antibody 9B11 (Cell Signal) at a 1 in 1000 dilution in blocking solution added to the surface of each transfected coverslip. Primary antibody incubated for 1 hour, after which primary antibody removed and coverslips rinsed 4 times in 2ml PBS.

200µl of secondary antibody Donkey anti mouse fluorescently tagged with Alexa 488 (Life technologies) in a 1:400 dilution in blocking media was added to the surface of each coverslip and was incubated for 1 hour in the dark. The coverslips were then washed four times in 2ml PBS, blot dried and mounted in 12µl of prolong gold for 12 hours. Mounted coverslips were imaged using a Leica immunofluorescence confocal microscope using Leica operating software.

Analysis of Lipid raft formation

HEK 293T cells were seeded in 6 well dishes containing coverslips. Coverslips soaked in Poly-L-Lysine (Thermofisher) for 3 hours and rinsed 4 times before use. Cells were grown in 2ml DMEM-10%FBS +Pen/Strep for 16 hours at 37 degrees and 5% CO_2 until 60 % confluent. Cells were transfected using TransIT – 293 transfection reagent (Mirus) according to manufactures protocol, with 5µg of desired plasmid.

Cells incubated for 48 hours post transfection at 37 degrees and 5% CO_2, culture medium removed and coverslips placed in 2ml of DMEM+FBS with 2µl of fluorescent cholera toxin B

(CT-B) conjugate labelled with Alexa 488 and incubated for 10 minutes at 4 degrees. After incubation coverslips washed 2 times in chilled 1x PBS and placed in 2ml of DMEM+FBS containing 10ul of Anti CT-B antibody, incubated at 4 degrees for 15 minutes. In order to allow visualisation of lipid raft domains.

Transfected coverslips placed in 2ml of 10%formalin-Phosphate buffered saline (PBS) for 10 minutes. Coverslips were rinsed in 2ml PBS twice and edges aspirate, after which 200µl of blocking solution (DMEM + FBS) added to surface of each coverslip and incubated for 20 minutes. 200µl of primary antibody Myc tag mouse monoclonal antibody 9B11 (Cell Signal) at a 1 in 1000 dilution in blocking solution added to the surface of each transfected coverslip. Primary antibody incubated for 1 hour, after which primary antibody removed and coverslips rinsed 4 times in 2ml PBS. 200µl of secondary antibody Donkey anti mouse fluorescently tagged with Alexa 594 (Life technologies) in a 1:400 dilution in blocking media added to the surface of each coverslip and was incubated for 1 hour in the dark. The coverslips were then washed four times in 2ml PBS, blot dried and mounted in 12µl of prolong gold for 12 hours. Mounted coverslips were imaged using a Leica immunofluorescence confocal microscope using Leica operating software.

VLP expression levels

HEK 293T cells were seeded in 6 well dishes containing coverslips. Coverslips soaked in Poly-L-Lysine (Thermofisher) for 3 hours and rinsed 4 times before use. Cells were grown in 2ml DMEM-10%FBS +Pen/Strep for 16 hours until 60 % confluent. Cells were transfected using TransIT – 293 transfection reagent (Mirus) according to manufactures protocol, with 5µg of desired plasmid.

Transfected cells incubated for 48 hours, after which supernatant extracted and concentrated to 30x concentration using Amicon Ultra 0.5 centrifugal concentrators (Millipore) as per manufactures specifications. Supernatant mixed with lysis buffer (Bolt LDS sample buffer (Invitrogen) and 500mM DTT) in a 1:5 lysis buffer: sample ratio.

Transfected cells were lysed using 250µl of Bolt LDS sample buffer, sheared using a needle and diluted in 1:10 dilution with lysis buffer solution. Samples heated at 90 degrees for 10 minutes in a drybath (Thermofisher). Samples run on a Bolt 4-12% Bis Tris plus 15 well precast gel (Novex) with sea blue 2 prestained ladder (Novex), run using a Bolt mini gel tank (Novex) as per manufacture protocol at 165 volt, 200 amps for 30 minutes. Gel electrophoresis transferred to membrane through iBlot dry blotting system (Invitrogen) as per manufactures protocol. Transferred membrane stained using western breeze chromogenic immunodetection kit (Invitrogen) as per manufacture protocol, stained with a primary antibody primary antibody Myc tag mouse monoclonal antibody 9B11 (Cell Signal) at a 1 in 1000 dilution. After which stained with a secondary antibody donkey anti mouse provided within the kit. Air dried for 12 hours and electronically scanned for analysis and saving using a standard computer scanner (Cannon).

Results

Neuraminidase is able to facilitate budding in a VLP system and influence VLP morphology

NA has been shown previously to be able to induce budding and formation of a VLP when expressed in a VLP system, it has also been shown that NA has a role in influencing VLP and virus morphology. To test this we examined the effects of NA of NA from a lab adapted spherical strain A/WSN/33 and a lab adapted filamentous strain A/Udorn/72 to see if NA is able to facilitate budding and confers any control of VLP morphology.

To investigate this plasmids containing either NA from A/WSN/33 or A/Udorn/72 were transfected into 293T HEK cells, incubated for 48 hours, fluorescently stained and imaged via immunofluorescence confocal microscopy to determine any budding activity and examine differences within VLP morphology.

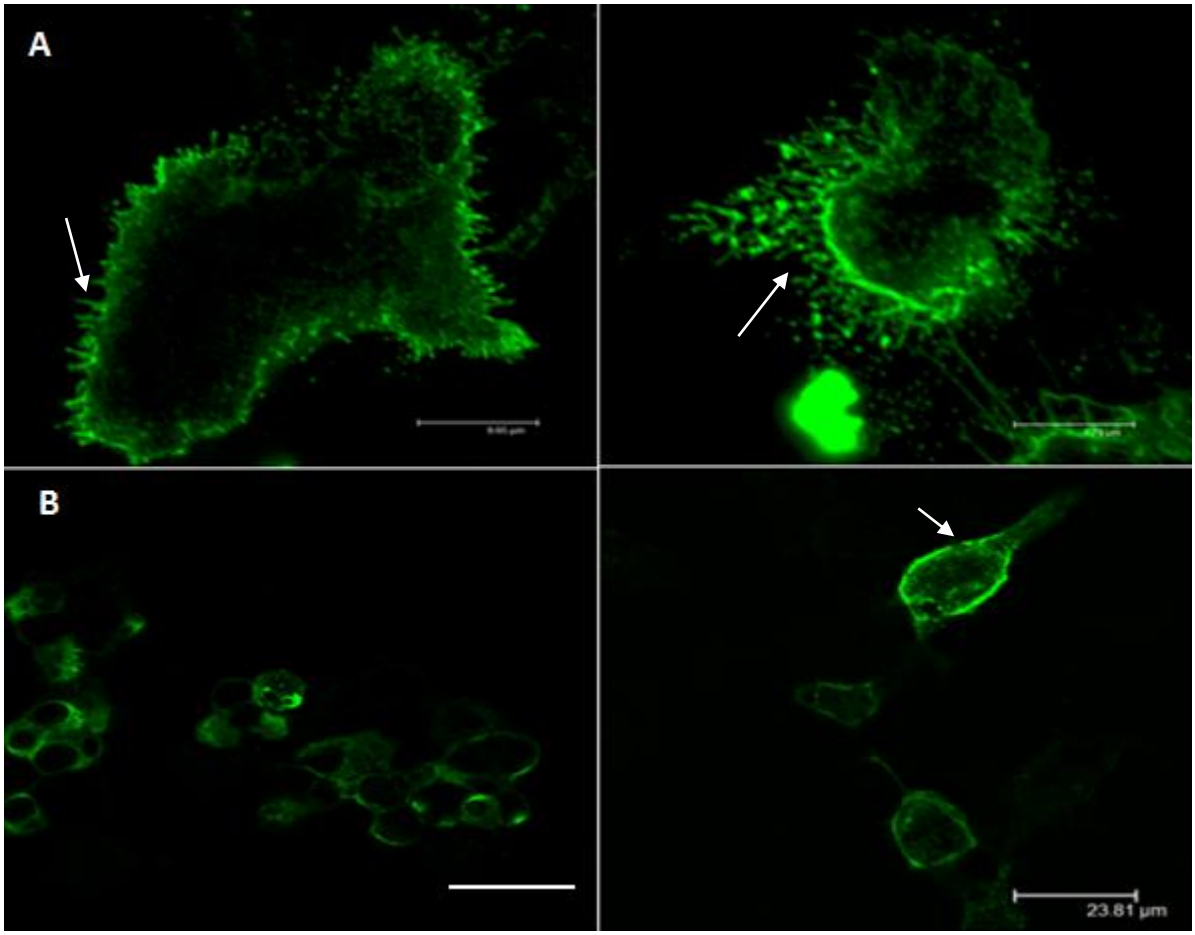

Fig 4: Comparison of HEK 293T cells transfected with NA from A/Udorn/72 and A/WSN/33 to assess NA's ability to facilitate VLP budding and examine the morphological differences between a primarily spherical and filamentous NA.

(A)Top panel showing HEK 293T cells transfected with NA of A/Udorn/72, transfected and incubated for 48hrs, labelled and stained with alexa 488 antibody imaged via confocal microscopy. Showing significant filament like VLP formations protruding form surface of transfected cells indicated by the white arrows showing filamentous VLP budding from cell membrane. Showing NA's ability to facilitate the budding and production of filamentous VLP's. Images taken by C Wilson of the Rossman laboratory, University of Kent.

(B) Bottom panel showing HEK 293T cells transfected with NA of A/WSN/33, transfected and incubated for 48hrs, labelled and stained with alexa 488 antibody imaged via confocal microscopy. Showing formation of puncta as indicated by white arrow showing dot like staining on surface of transfected cells indicating the production of spherical VLP's. Scale bar indicating 21µm.

The results of this investigation showed as already suggested that NA is able to facilitate budding in a VLP system (Fig 4). Confocal imaging of NA of A/WSN/33 (Fig 4A) resulted in formation of bulges in cell membrane and fluorescent dot like staining on the cell surface known as puncta[32] indicating the formation and production of spherical VLP's. Confocal imaging of NA of primarily filamentous strain A/Udorn/72 resulted in budding of VLP from

surface of transfected cells (Figure 4B), but also revealed VLP's with a distinctly filament like structure seen widely budding from surface of cells across all transfected samples as we previously seen within our laboratory (data not shown).

Alterations in the transmembrane domain of neuraminidase result in changes in virus like particle morphology

As shown in figure 4 NA is able to confer varying morphological traits when expressed, previous research [28] has also shown that mutations within the TMD can result in differing changes in virus morphology. To elucidate if the TMD is responsible for morphological characteristics of NA or confers any ability to alter membrane curvature, PCR overlap cloning was used to replace the TMD of A/WSN/33 NA (WT WSN) with the TMD of the primarily filamentous pandemic A/California/09 NA (WSN-PN1) (Gifted by Dr R Daniels, University of Stockholm). A/California/09 strain was chosen as both are N1 subgroup of NA, but have various differences in amino acid sequence structure of their TMD. The TMD of A/California/09 has also been found to have a higher hydrophobicity and weaker polar interactions compared to that of other NA N1 strains such as A/WSN/33[30].

Both pcDNA3.1A-myc-his tagged plasmids were transfected into 293T HEK cells, incubated for 48 hours, stained and imaged via immunofluorescence confocal microscopy to analyse VLP morphology. Repeats of transfection of WT WSN NA through confocal microscopy (Fig 5) confirmed the ability A/WSN/33 NA to induce budding and produce spherical VLP's, through strong indication of puncta like staining on the surface of transfected cells. Examination of the replacement of TMD of A/WSN/33 NA with that of A/California/09 NA (WSN-PN1) through confocal imaging revealed the production of filament like VLP's on the surface of the transfected HEK 293T's.

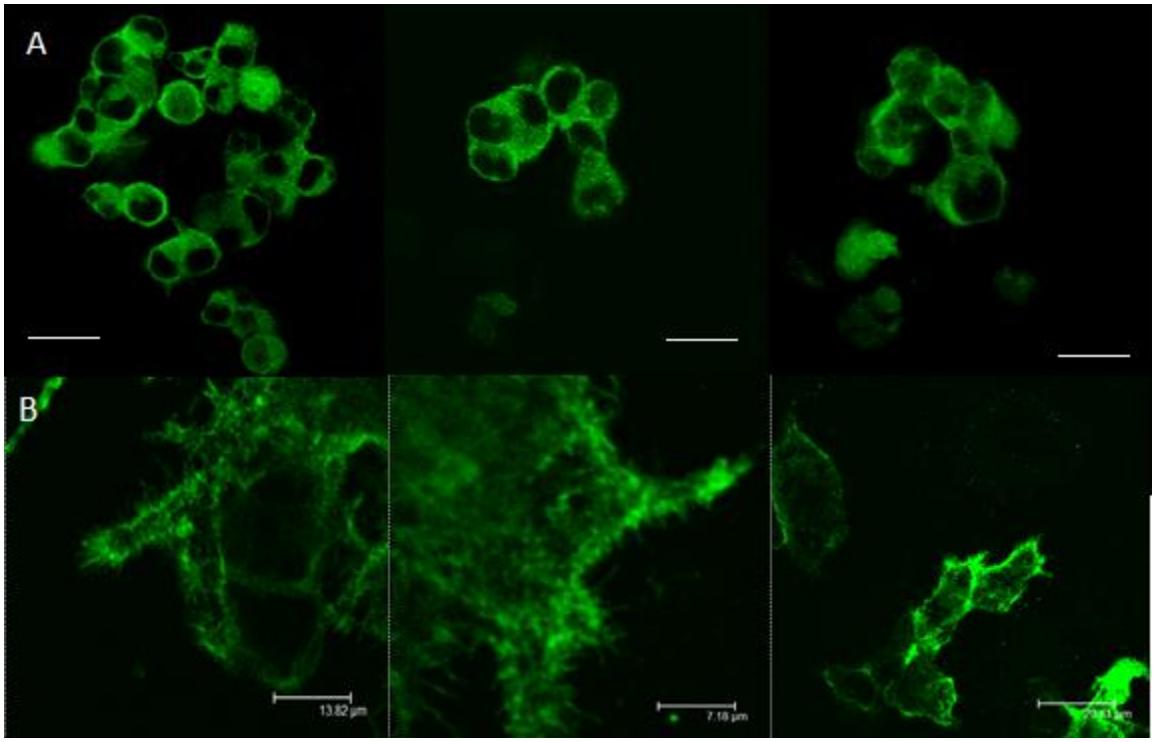

Fig 5: (A) top row showing HEK 293T cells transfected with plasmid vector pcDNA3.1A myc-his tag expressing A/WSN/33 NA, incubated for 48 hours at 37 degrees and 5% CO_2, stained, fixed and imaged by immunofluorescence confocal microscopy. Showing characteristic puncta like staining on surface of transfected cells indicating the production of spherical virus like particles. Scale bar (white) of 23µm.

(B) Bottom row showing HEK 293T cells transfected with plasmid vector pcDNA3.1A myc-his tag expressing A/WSN/33 NA with the TMD of A/California/09 strain (WSN-PN1), incubated for 48 hours at 37 degrees and 5% CO_2, stained, fixed and imaged by immunofluorescence confocal microscopy. Showing long filament like particles protruding from the surface of transfected cells. These filament like structures are characteristic and similar to that in morphology of confirmed filamentous virions and VLP's seen in previous literature.

Differing hydrophobicity of fully assembled transmembrane domain do not alter virus like particle morphology.

Recent research [30] has suggested that the NA TMD interactions are linked to hydrophobicity of the TMD residues in terms of TMD assembly and interaction of polar faces with the TMD. To explore the possibility that these specific polar faces and the hydrophobicity of NA TMD alter interactions and if these interactions have any effect of VLP morphology, several plasmid constructs kindly provided by Robert Daniels at University of Stockholm were utilised. Three distinct sets of mutations were made in the NA TMD residues responsible for three distinct polar faces of WSN-PN1 plasmid through PCR overlap cloning. Mutations were

made through alanine substitutions in TMD in the residues responsible for conserved adjacent A polar faces (WSN-PN1- Δ-A), E polar face (WSN-PN1- Δ-E) and a final mutation made with both A and E polar face mutations (WSN-PN1- Δ-AE), shown in supplementary data (S3).

The aim of these mutations were to create varying differences in A/California/09 transmembrane assembly through mutation of polar residues and designed to bring the polarity, assembly and strength of interaction of A/California/09 TMD to a similar levels as that of A/WSN/33.

The results of these experimentations (Figure 6) by analysis through confocal microscopy revealed that although replacement of the transmembrane domain of primarily spherical strain with that of a filamentous strain yielded alterations in morphology and production of filamentous VLP's. Mutations within the A (WSN-PN1- Δ-A), E (WSN-PN1- Δ-E), and both A and E face (WSN-PN1- Δ-AE) designed to alter TMD assembly and strength of interaction to that N1 and other NA sub types, did not yield any differences in morphology (S1, S2). As seen with expression of WSN-PN1 there was formation of filament like structures from all polar mutations. Further analysis and scanning of filamentous like formations of WSN-PN1- Δ-A, WSN-PN1- Δ-E, WSN-PN1- Δ-AE (Figure 6) revealed no significant differences within structure or morphology of formed filament like structures across varying polar mutation and full TMD swap WSN-PN1.

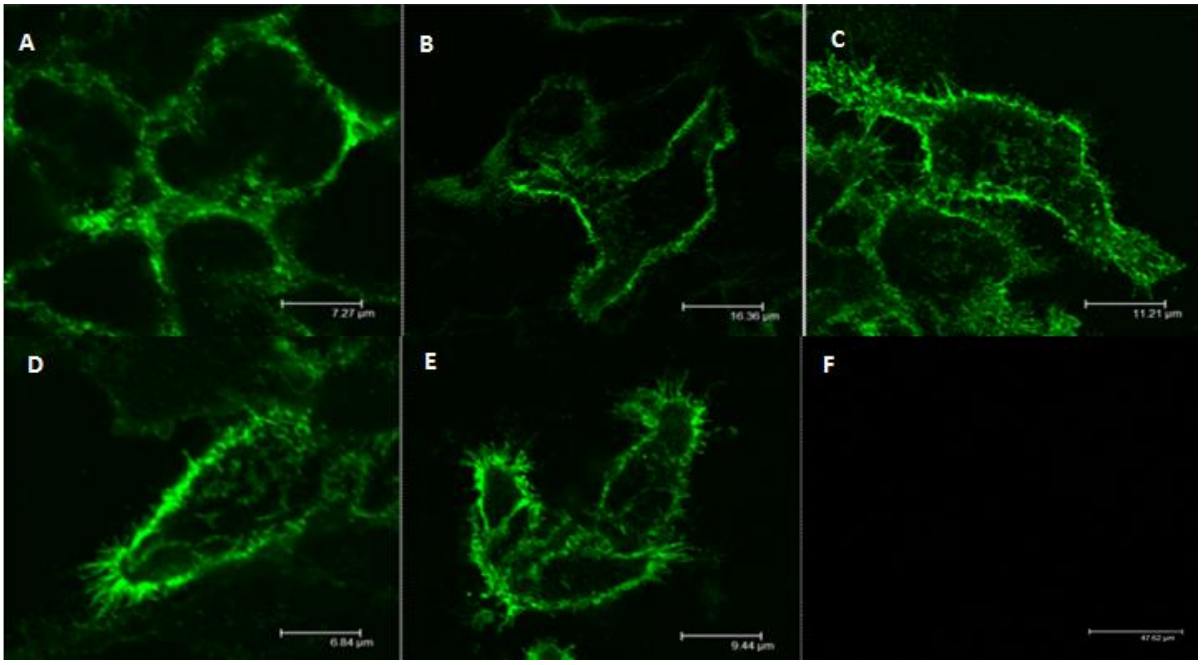

Fig 6: Confocal analysis of HEK 293T cells transfected with pcDNA3.1A myc-his tag plasmids vectors, incubated for 48 hours, stained with alexa 488 antibody, fixed and imaged via immunofluorescence confocal microscopy. (A) Showing wild type WSN NA (WT WSN) expression forming spherical virions. (B) Showing expression of WSN NA with TMD of pandemic 09 strain (WSN-PN1), forming filamentous virus like particles. (C) Showing WSN NA with TMD of pandemic 09 strain with alanine substation in the residue encoding for the conserved A polar face.(D)showing WSN NA with TMD of pandemic 09 strain with alanine substation in the residue encoding for the conserved E Polar face. (E)Showing WSN NA with TMD of pandemic 09 strain with alanine substation in the both residues encoding for the conserved A and E polar faces. With (C), (D) and (E) forming filament like structures similar in size and morphology to that of WT pandemic 09 residue (B)(WSN-PN1) with no significant difference in morphology being found. (F) Showing control sample of empty pcDNA3.1A vector being transfected and stained to same conditions as per other experiments.

Analysis of lipid raft formation

Alterations within the TMD although seemingly able to alter membrane curvature and induce budding of filamentous VLP's, the hydrophobicity of the TMD does not seem to be responsible alone for the alterations in morphology. It has previously been shown that concentration of lipid raft domains within a virally infected cell play an important role in the initiation of membrane curvature by HA and NA[14]. We hypothesised that mechanisms behind filament formation may affect lipid raft formation within the transfected cell, we

also set out to examine if varying alterations affecting TMD assembly resulted in differences in the insertion of TMD into the cell membrane.

To do this we utilised cholera toxin b subunit, which binds GM1 lipids found in lipid raft domains and allows cross linking with a fluorescent antibody to stain transfected cells after a 48 hour incubation period and imaged via confocal microscopy (Fig 7).

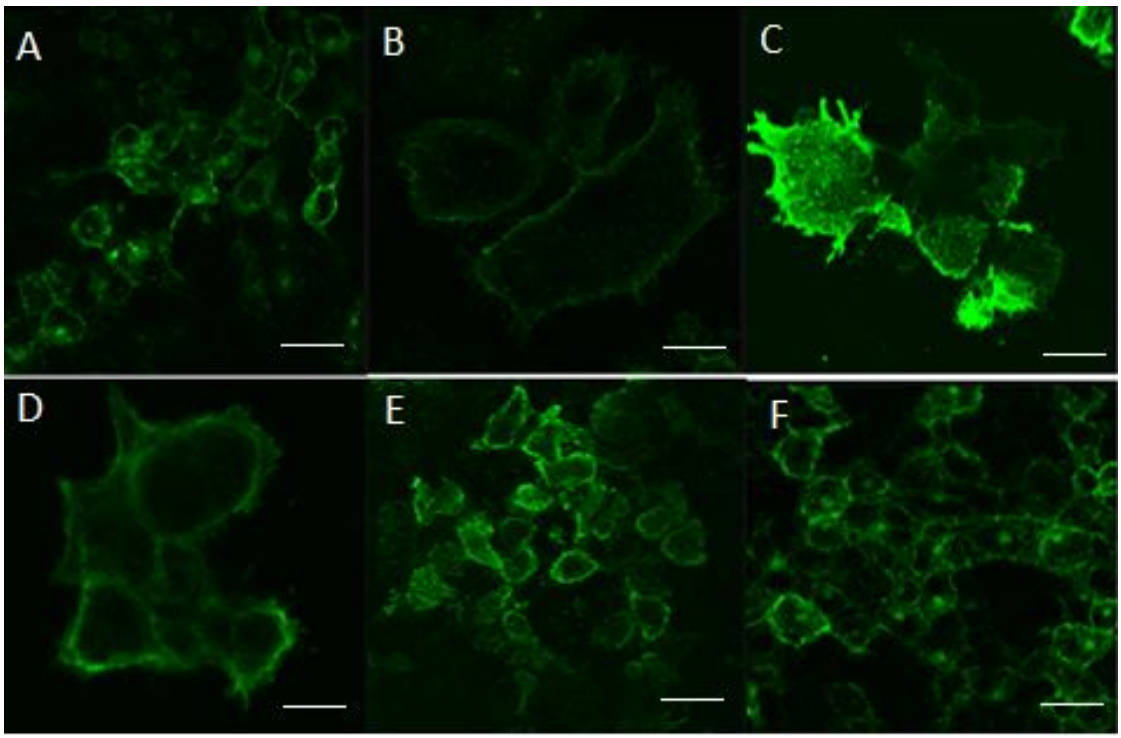

Fig 7: Confocal imagery of lipid raft formation by transfection of plasmid vectors both WT and TMD mutations into 293T HEK cells, incubated for 48 hours and stained with alexa 488 fluorescently labelled cholera toxin B crosslinked antibody, imaged through confocal microscopy. (A) Lipid raft staining of WT WSN NA Showing dense staining of lipid raft domains toward out membrane, with strong puncta like staining seen on surface cell. Scale bar represents 22µm. (B)Lipid raft staining of WSN-PN1, showing diffuse level of staining with stronger localisation of lipid raft domains on out cell membrane, but centrifugal pattern of intracellular staining with cell cytoplasm. Scale bar representing 14µm. (C) Lipid raft staining of WSN-PN1-Δ-A, showing two types of observed pattern of staining. High intensity localised staining in cell membrane, budding filaments and localised areas within the cytoplasm of transfected cell. The other observed pattern being similar to WSN-PN1 with more diffuse intracellular staining and more intense staining on cell membrane. Scale bar representing 18µm. (D) lipid raft staining of WSN-PN1- Δ-E, showing a conserved pattern of diffuse intracellular staining, with more concentrated staining on the cell surface. Scale representing 13µm. (E) Lipid raft staining of WSN-PN1- Δ-AE, Showing similar results to that of WSN-PN1 and WSN-PN1- Δ-E with wide spread intracellular staining and more concentrated lipid raft formation on cell membrane and budding filaments. Scale bar representing 20µm. (F) lipid raft staining of empty vector pcDNA3.1A (Invitrogen) control, scale bar representing 20µm.

Examination of lipid raft formation (Figure 7) revealed several differences in raft formation amongst WT and varying mutations. WT NA showed distinct localisation of raft formation within puncta formations within the plasma membrane. NA mutants WSN-PN1- Δ-E, PN1-WSN- Δ-AE showed similar levels of raft localisation both within filament formations from the plasma membrane and significant intracellular staining of lipid raft domains. WSN-PN1-Δ-A showed two distinct levels of raft formation, one similar to that of WSN-PN1- Δ-E and AE mutations. The other with significant higher levels of staining and raft formation both in budding filaments and intracellularly, in a centrifugal pattern towards the cell membrane.

Neuraminidase is capable of causing concentration of lipid raft domains

Based on various concentration of lipid raft domains (Figure 7) and previous research [5,14] we set out to test the current hypothesis that NA is able to concentrate lipid raft domains causing creation of these viral budozones and initiating membrane curvature by analysing NA's ability to localise to high lipid areas. Transfected HEK 293T were dual stained with antibodies to both lipid raft domains and NA to allow the visualisation of both lipid raft domains and NA simultaneously to allow analysis of co-localisation.

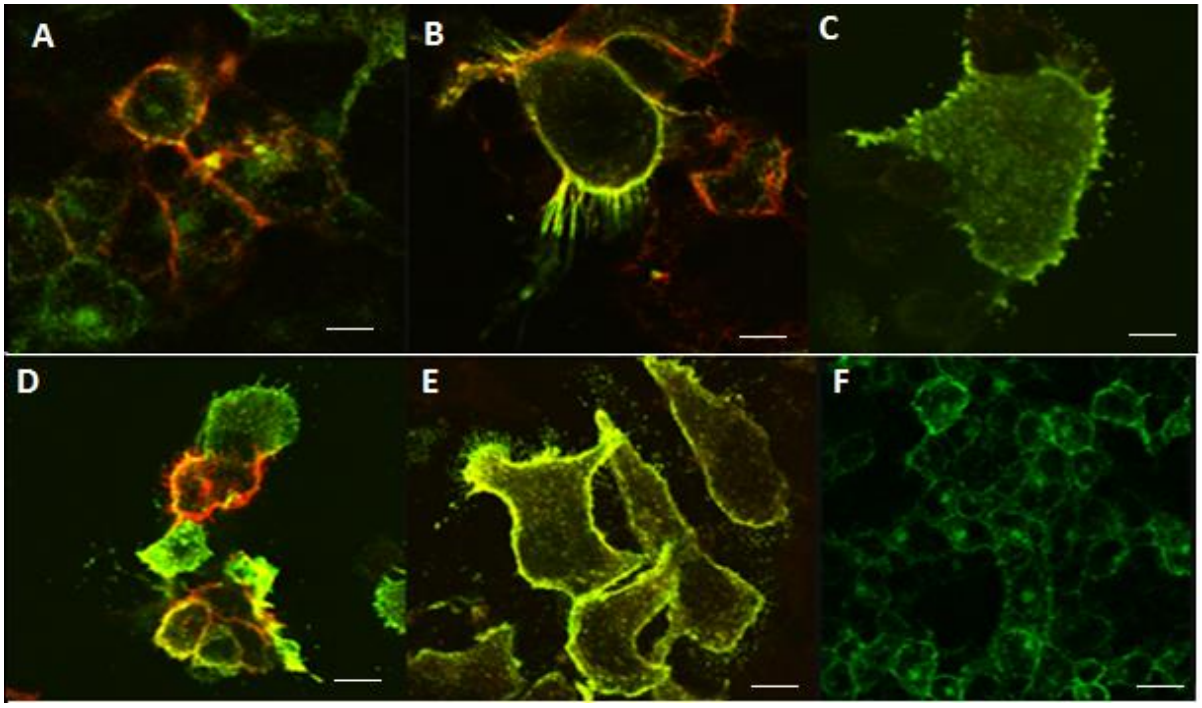

Fig 8: Analysis of co-localisation between lipid raft domains and NA through confocal imagery of HEK 293T cells that had been transfected with plasmid vectors, incubated for 48 hours and dual stained with alexa 488 fluorescently labelled cholera toxin B conjugate to image lipid raft formations (Shown in green). And alexa 594 fluorescently labelled donkey anti mouse antibody to image NA (Shown in red) to analyse co-localisation of NA and lipid raft domains (Shown in yellow).

(A)HEK 293T cells transfected with plasmid vector expressing WT WSN NA. Confocal imaging revealing circular punctate like areas of co-localisation on cell membrane. Along with expression of NA and lipid raft formation both on cell membrane and intracellularly around cell membrane. Scale bar indicating 25µm.

(B) HEK 293T cells transfected with plasmid vector expressing WSN-PN1 NA. Confocal imaging showing extensive co-localisation of NA to lipid raft domains, including extensive co-localisation budding filamentous VLP's. Scale bar indicating 21µm

(C)HEK 293T cells transfected with plasmid vector containing WSN-PN1- Δ-A NA. Confocal imaging revealing extensive co-localisation of NA to lipid raft domains around cell membrane and in budding filamentous VLP. Also showing extensive co-localisation of NA and lipid raft domains within cytoplasm of transfected cells. Scale bar representing 15.4µm

(D) HEK 293T cells transfected with plasmid vector containing WSN-PN1- Δ-E NA. Confocal imaging revealing extensive co-localisation of NA and lipid raft domains. Also intracellular co-localisation, along with significant expression shown by large volume of red staining similar to that of WSN-PN1(with unmutated A/CAL/09 TMD) possibly indicating similar insertion and hydrophobic interaction to that of WSN-PN1.

(E) HEK 293T cells transfected with plasmid vector containing WSN-PN1- Δ-AE NA. Confocal imaging showing both co-localisation on cell membrane and intracellularly similar to that of WSN-PN1, but with more extensive localisation of NA and lipid raft domains on cell membrane.

(F) HEK 293T cells transfected with empty pcDNA3.1A plasmid vector as a control. Showing no NA and similar lipid raft formation to that of untransfected HEK cells.

The results (Figure 8) showed that both spherical WT WSN NA and filamentous producing mutants showed strong indication and evidence of co-localisation staining between NA and lipid raft formation. This experiment also further showed the diffuse pattern of staining seen previously (Figure 7), with WT WSN NA demonstrating dotted puncta like staining.

WSN-PN1- Δ-A, -E, and –AE showing diffuse intracellular staining and more intense staining within the plasma membrane and high localisation within forming filaments, as well as a strong presence of co-localisation of NA and lipid rafts intracellularly. Compared to WSN-PN1 which showed co-localisation of NA and lipid raft domains, but very little intracellular co-localisation, as well as significantly cells lipid raft formation within the transfected cells.

The ability of NA to facilitate membrane scission and the release of budding virus like particles

NA is seemingly able to produce both filamentous and spherical VLP's when transfected in HEK 293T cells. Previous work form our laboratory has indicated to some extent that viral proteins such as HA when transfected in a VLP and examined through transmission electron microscopy (TEM) are able to seemingly facilitate membrane scission and release budded VLP's (Dr J Rossman, personal communication, May 2014) in the supernatant of transfected cells (data not shown).

Although it is unknown if NA is able to induce membrane scission of budding virions especially filamentous virions or virus like particles. This is partly due to the process of purification required for the analysis of supernatant under TEM, this is due to fragility of filamentous VLP's, which under the required concentrations result in destruction of

filamentous structures and leading to formation of artefacts and inconclusive data as shown in supplementary figure 4 (S4).

To overcome this supernatant and cell lysate were taken from HEK 293T cells that had been transfected with plasmid vectors WT WSN, WSN-PN1, WSN-PN1- Δ-A, WSN-PN1- Δ-E, WSN-PN1- Δ-AE and incubated for 48 hours. Examined western blot with the aim to analyse NA levels in the cell supernatant under the hypothesis that if NA was able to facilitate membrane scission, and release of VLP's there would be significant release of NA, with the cell lysate being used to measure comparable levels and indication of NA levels within the cell.

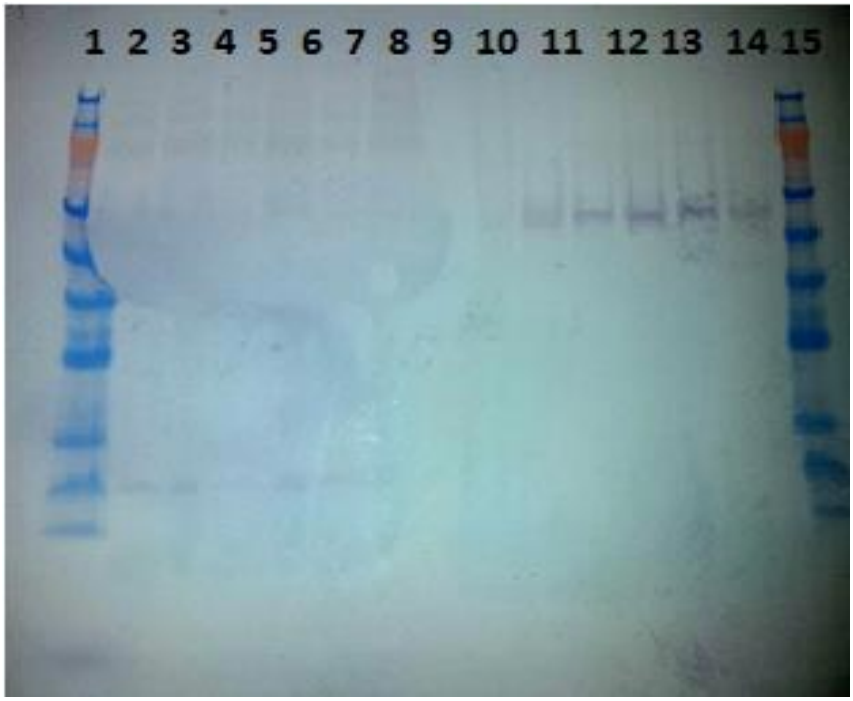

Fig 9: Comparison of NA levels within the supernatant and cell lysate of transfected HEK 293T cells. Break down as follows lanes 1 and 15 showing sea blue 2 prestained ladder (Novex). Lanes 2 to 8 showing samples taken from cell supernatant, showing expression of WT WSN(2) and (3), WSN-PN1(4) and (5), WSN-PN1- \Delta-A (6), WSN-PN1- \Delta-E(7), WSN-PN1- \Delta-AE (8). Untransfected HEK 293T control sample (9).

Lanes 10 to 14 show samples taken from cell lysate, WT WSN cell lysate (10), WSN-PN1 cell lysate(11), WSN-PN1- \Delta-A cell lysate (12), WSN-PN1- \Delta-E cell lysate(13), WSN-PN1- \Delta-AE cell lysate (14).

Cell lysate as shown in lanes 10 to 14 shows expression of NA as expected from confocal analysis. Cell supernatant shows no distinctive pattern of banding indicating either an issue with purification and concentration of VLP's or possibly that NA is unable to facilitate the release of budding VLP's.

The result of this experiment (Figure 9) showed expression of NA within the cell lysate confirming NA within the transfected cell and what had been seen previously through confocal analysis. Analysis of cell supernatant revealed partial staining or sheet of staining when imaged revealing no conclusive evidence of VLP release within the cell supernatant, which as shown in supplementary data (S5) is repeatedly seen.

Loss of neuraminidases enzymatic head domain results in alteration of virus like particle morphology

Alterations within the transmembrane domain as shown can result in changes in VLP morphology causing the production of filamentous VLP's (figure 4 and 5). It is also thought that alteration in polarity and structure of NA result in changes amongst assembly of TMD, which in turn results in changes to assembly of NA and its insertion into plasma membrane[30,31].

The exact mechanism behind NA's ability to create both filamentous virion and virus like particles is currently unknown[14]. We hypothesised that filamentous VLP formation may be dictated by either the activity or the structure of enzymatic head domain or possibly through the insertion of the TMD and its interactions with the plasma membrane.

To test this we utilised a series of plasmid constructs NA76- ΔeltaG+1.3 pcDNA kindly produced by R Daniels at University of Stockholm. These plasmids contained only a 76 amino acid ectodomain containing variable stalk length but missing the enzymatic head region (Figure S6). These plasmids consisted of WT WSN-PN1 as seen previously and several other plasmids which has been created with amino acid substitutions and replacements within the highly conserved N terminus or cytoplasmic tail. These mutations consisted of varying deletions and substitutions with the N terminus as illustrated in supplementary data (Figure S6).The aim of this was to image and compare the expression and localisation of NATMD to assess if even with mutations within the cytoplasmic tail (CT) the TMD is able to facilitate insertion into the plasma membrane. The other aim of this experiment was to see if the insertion of the TMD alone is sufficient to induce VLP budding or alter membrane curvature.

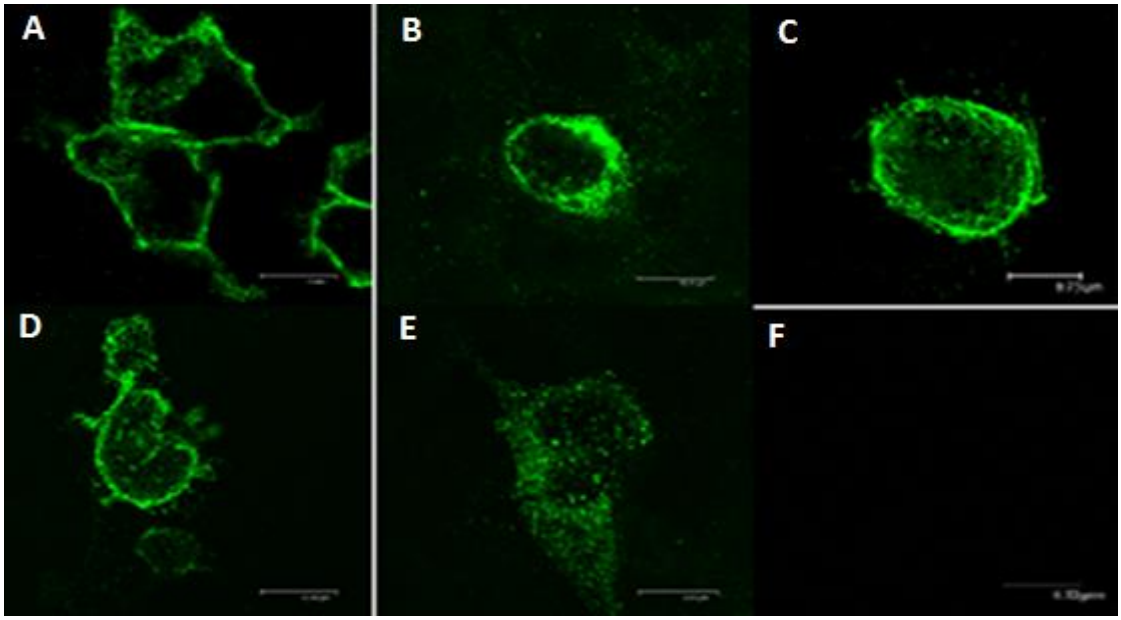

Fig 10: Confocal images of comparison of TMD insertion and alterations to morphology of WSN-PN1 and M(B), MK(C), MAK(D) and MAA(E) cytoplasmic tail mutations expressed in HEK 293T cells, transfected and incubated for 48 hours and stained with alex 488.

(A)HEK 293T cells transfected with plasmid vector expressing WSN-PN1 NA containing only the cytoplasmic tail (CT), TMD and stalk domain of WSN-PN1 NA. Showing expression of NA both intracellularly and with evidence of insertion of NA in the plasma membrane of transfected cells, no evidence of budding either spherical or filamentous noted

(B) HEK 293T cells transfected with plasmid vector expressing WSN-PN1 NA (M) with deletion of cytoplasmic tail containing only a singular Methionine (M) residue. Showing successful insertion of NA into plasma membrane and expression but no evidence of membrane scission of budding.

(C) HEK 293T cells transfected with plasmid vector expressing WSN-PN1 NA (MK) with residue deletions within the CT, containing only M and Lysine (k) residues. Showing successful insertion of NA, but with comparable levels of budding to that of M and WSN-PN1 mutants.

(D) HEK 293T cells transfected with plasmid vector expressing WSN-PN1 NA (MAK) substitutions of CT residues 2-4 with alanine residues (MAK). With comparable levels of insertion to that of M, MK mutations.

(E) HEK 293T cells transfected with plasmid vector expressing WSN-PN1 NA (MAA) with substitutions of CT residues 2-5 with alanine residues. With comparable levels of insertion to that of M, MK mutations, although a small proportion transfected cells expressed higher amount of intracellular staining compared to other mutations imaged.

(F) Control sample showing empty vector pcDNA3.1A transfected in HEK 293T cells under same conditions as other mutations, showing no fluorescence when imaged via confocal microscopy.

The results of this experiment showed (Figure 10) that seemingly even with mutations within the CT of NA the TMD is able to insert and be expressed within the plasma

membrane of transfected cell, with no comparable differences in expression between WT CT and various mutations being noted.

The results also showed that despite the TMD is able to insert and be expressed within the cell membrane of transfected cells, there was a loss of filament morphology across all the transfected cells including WT WSN-PN1 and varying CT mutations (Figure S6). Although there is evidence of puncta like staining the lack of bulging of membrane as previously shown when spherical budding occurs suggest a lack of budding and alteration of membrane curvature. This indicates that the enzymatic head domain may be responsible for the initiation of membrane curvature and facilitating virion or VLP morphology.

Discussion

In this research project we researched the role of NA in the process of budding and its involvement in virion and VLP morphology. More specifically the role the TMD of NA has on membrane curvature and the assembly of NA.

Neuraminidase transmembrane domain may possess conversed features which influence virus morphology

The current mechanisms behind budding of the influenza A virus are currently unknown. The current model of budding[14] suggest that it is a multi-step process that relies on the interactions of several of viral proteins NA, HA, NP, M1 and M2 to facilitate the assembly and production of mature influenza virions. In terms of the production of either filamentous or spherical virions many of the main viral proteins have been implicated in influencing virus morphology such as M2[25,34,35], NA and HA[5,13,23,24], M1[21,22].

Our research has shown that NA taken from either a virus with primarily spherical or filamentous morphology, conserves this morphology when expressed in a VLP system (Figure 4). When examined further (Figure 5) we have shown the TMD of primarily filamentous strain such as that of A/California/09 when substituted into a primarily spherical producing NA results in alteration in morphology and the production of primarily filamentous VLP's.

The ability of the TMD to alter morphology may be due several possible reasons, one is that the TMD has been implicated in the assembly of NA through anchoring NA to membrane during assembly[31]. It could be through this anchoring of the ectodomain to the plasma membrane that allows a stable platform of which NA to fully assembly. Depending on the strength and stability of this binding dictated by the properties of the TMD, could in turn alter the physical properties and strength of assembly of the enzymatic head domain and

variable stalk region. This difference in assembly could lead to structural difference such as differing structural and enzymatic activity.

Another possibility is that the structure of the TMD it's self and the insertion of the TMD into the plasma membrane may mediate the membrane curvature needed to initiate the formation of filamentous virions.

Previous research [30,31] has shown the structure of the transmembrane domain more specifically the position of various polar faces within the structure of the TMD leads to alterations in the polar activity and ultimately the hydrophobicity of the TMD (S1,S2). Leading to varying differences in the strength of interaction between the TMD and the plasma membrane. This strength of reaction may also dictate whether the TMD is able to insert and interact strongly enough to initiate membrane curvature and stabilise the budding virion to allow the production of filaments. Although our experiments showed that when transfected in a VLP system, NA containing only the CT, TMD and variable stalk region is not sufficient to induce membrane curvature, but shows no conclusive evidence of VLP production. This may be due the TMD it's self not being solely responsible for the alteration of membrane curvature and VLP production, NA may require the enzymatic head domain or full NA structure in order to insert into the membrane with the required force to generate sufficient membrane curvature. This may be also due to the lack of enzymatic head domain, as it is required for the concentration of lipid raft domains in the plasma membrane and the theorised first step and initiation the of budding process. The lack of the enzymatic head domain and loss of concentration of lipid raft domains likely meant that as this concentration of lipid was missing, the initial alteration in membrane curvature thought to be required for the start of the budding process was absent. Assuming this lipid raft concentration if required, it is possible that the insertion of the TMD into the plasma

membrane relies on this initial curvature in order to generate enough force of which to facilitate the primary stages of budding and influence virus morphology.

Further research is need to elucidate the mechanisms behind which the TMD influences morphology into either structural confirmation of NA such as enzymatic activity or in regards to the insertion capabilities of NA. At the time of writing, our lab is undertaking a data mining project designed to compare the residue structures of the NA TMD's of primarily spherical and filamentous strains and comparing residue differences, alongside examining if previous literature has found residue mutations with the TMD which seemingly alter the enzymatic activity NA.

More research is also needed to analyse the effects of the TMD on enzymatic head domain to rule out this theory and possibility of alterations. This could be achieved through reverse genetic mutations of NA with varying TMD mutations and measuring of enzymatic, and crystallography data of NA mutations as well as mapping sequential and functional differences within the head domain.

Failure of western blot analysis to determine the ability of neuraminidase to facilitate the release of budding virus like particles

The longest known role of NA is that it is able to cleave sialic acid residues from the cell surface of infected cells in order to prevent coagulation of budding virions and facilitate the release of mature virions from the cell surface. We hypothesised that because of this in a VLP system NA should in theory be able to facilitate the release of VLP provided it can induce sufficient membrane curvature to allow pinching off and release of new budding

virions. A role that in the release of mature virions in a live model is thought to be facilitated by M2.

Due to previous experimentation through TEM in our laboratory, we found that the concentration process required to extract and image cell supernatant for the release of filamentous VLP's resulted in inconclusive data (data not shown). This was thought to be due to the fragility of filamentous VLP, with the concentration and processing steps required for TEM resulting in the destruction of filamentous VLPs and production of large amounts of artefacts providing inconclusive data (S4).

Despite alteration to methodology for a gentler concentration, our aim to explore NA VLP release through analysis of NA in the cell supernatant through western blotting proved to also yield largely inconclusive data. This could be due to the concentration and spin methodologies used result in the destruction of filaments and improper concentration of VLP's, a step which is currently being tested in our laboratory is the use of a sucrose gradient purification system, allowing gentler and more efficient concentration of VLP's. Although the data shows clear expression of NA from the cell lysate, indicating the expression of NA in transfected cells, the data shows no conclusive evidence of NA within the supernatant of transfected cells. With some sporadic staining seen, but unclear if this staining is due to over staining or as a result of the destruction of budding filaments caused by the concentration of supernatant, resulting in fragmentation of VLP's leading to this sheet like staining and no clearly defined banding patterns. With these results being observed repeatedly through various rounds of concentration and western blot analysis (S5).

It could also stand to reason that either the level of VLP expression is at low and undetectable amount or the concentration level required is beyond the range of current concentration and western blot method to allow adequate concentration of sample and detection of NA.

It may also be possible that although NA is able to significantly alter membrane curvature it may not generate enough force required to allow the release of budding VLP's and may require the interaction of other viral proteins such as M1 and M2 in order to facilitate negative membrane curvature and required force to allow the pinching and release of budding virion.

Further research is needed into the ability of NA to facilitate the release of budding VLP's and the kinetics that required to allow this process to happen.

Neuraminidase enzymatic head domain is seemingly required to facilitate budding in a VLP system

As we have shown NA is seemingly and quite complexly involved in the budding process, the exact extent of which is currently unclear. We have shown in this research project that the TMD as previously seen [28,29] is able to alter morphology. Although the mechanism of which is unclear, our research has shown that when expressed singularly the TMD is not able to alter membrane curvature and is seemingly unable to facilitate budding. The formation of puncta like staining, but lack of membrane curvature or bulging suggests that TMD alone is not able produce spherical or filamentousVLP's. Although further examination through expression and TEM studies is required to complete confirm the absence of spherical VLP's from these experiments.

On the surface these results suggest that the enzymatic head domain is required in order to facilitate budding. As previously mentioned this may be due to a number of factors such as the head domain giving the required strength need by NA to insert effectively into membrane or being required to concentrate lipid raft domains to allow budding process to begin. Interestingly it may possible that during assembly of NA mediated by the TMD alterations within stalk height or ectodomain itself, caused by the TMD may result in alterations in the structure and enzymatic activity of NA which results in different morphology.

Neuraminidase is able to strongly localise to lipid raft domains during budding

The current theory on the process of influenza virus budding and the interactions of viral proteins in budding suggests that HA[36] and to a lesser extent NA is able to cause the concentration of lipids into lipid raft domains, thought to be responsible for the initiation of membrane curvature and starting the budding process. Previous studies have suggested that NA is able to localise and cause concentration of lipid raft domains although within the field there is a significant divide in the exact extent NA is thought to be able to contribute to this process

We have shown (Figure 8) that when expressed in a virus like particle system that NA is able to strongly co-localise to lipid raft domains both in the production of filamentous and spherical VLP's. Providing strong evidence to support the current theory of budding that NA is able to localise and concentrate lipid raft domains.

Our results also showed varying difference in lipid raft interactions particularly amongst NA TMD mutants WSN-PN1- Δ-E, WSN-PN1- Δ-AE which showed strong intracellular localisation of lipid raft domains. This more intense staining of lipid raft domain both on plasma

membrane and intracellularly may be due to the strength of interaction of the TMD with the plasma membrane. The differences in polarity, structure and position of the polar faces may alter the strength of insertion and interaction of the TMD with membrane due to differing hydrophobicity of the TMD as currently thought [30].

Further research is needed particularly in the area of time lapse confocal microscopy examining NA formation and lipid raft concentration, along with examination of raft formation and lipid concentration when expressed in NA mutants lacking enzymatic head domain will help confirm and provide further evidence of NA's ability to concentrate lipid raft domains.

Impact of this research project

Overall this research project produced several key findings which add to the current cannon of knowledge surrounding the process of budding and morphology of the influenza A virus. We have confirmed that as previously thought NA seemingly doe play a role in morphology of the influenza A virus and there is a strong correlation between NA and concentration of lipid raft domains supporting the current work around the process of budding.

We have also shown that the TMD is able to alter morphology, with the TMD seemingly being able to conserve and confer filament morphology and that both the both head domain and TMD play a role in budding. This research in turn will have an importance in a mixture of areas such as pharmaceutical industry more specifically production of seasonal influenza vaccine. Where the random production of filamentous virions affects and disrupts manufacture and purification of vaccine leading loss of time and money. As well as further adding to the current base of knowledge surrounding the influenza virus.

Acknowledgments

I would like to thank Dr Rossman for help, guidance and support in carrying out this research project. Along with members of the Rossman lab past and present, Chris, Aga, Matt, Basma and Alex for support and sharing of ideas and trouble shooting. Mr Ian Brown, microscopy facilitates manager at University of Kent for training and guidance on confocal microscopy. This research was support by grants from European research council (ERC) and Medical research council UK (MRC).

References

1. WHO | Influenza (Seasonal). at <http://www.who.int/mediacentre/factsheets/fs211/en/>

2. Carrat, F. & Flahault, a. Influenza vaccine: the challenge of antigenic drift. *Vaccine* **25,** 6852–62 (2007).

3. Xu, R., Ekiert, D., Krause, J. & Hai, R. Structural basis of preexisting immunity to the 2009 H1N1 pandemic influenza virus. *Science (80-.).* **328,** 357–360 (2010).

4. Taubenberger, J. K. & Morens, D. M. 1918 Influenza: the mother of all pandemics. *Emerg. Infect. Dis.* **12,** 15–22 (2006).

5. Chen, B. J., Leser, G. P., Morita, E. & Lamb, R. A. Influenza virus hemagglutinin and neuraminidase, but not the matrix protein, are required for assembly and budding of plasmid- Δerived virus-like particles. *J. Virol.* **81,** 7111–7123 (2007).

6. Varghese, J. N., Laver, W. G. & Colman, P. M. Structure of the influenza virus glycoprotein antigen neuraminidase at 2.9 Å resolution. *Nature* **303,** 35–40 (1983).

7. Elleman, C. J. & Barclay, W. S. The M1 matrix protein controls the filamentous phenotype of influenza A virus. *Virology* **321,** 144–153 (2004).

8. Zebedee, S. L. Structure and function analysis of the influenza A virus M2 protein. *Disertation Dr. Philos. Northwest. Univ. Evanston, IL.* (1988).

9. Czabotar, P. E., Martin, S. R. & Hay, A. J. Studies of structural changes in the M2 proton channel of influenza A virus by tryptophan fluorescence. *Virus Res.* **99,** 57–61 (2004).

10. Hay, A. J., Lomniczi, B., Bellamy, A. R. & Skehel, J. J. Transcription of the influenza virus genome. *Virology* **83,** 337–355 (1977).

11. Zamarin, D., Ortigoza, M. B. & Palese, P. Influenza A virus PB1-F2 protein contributes to viral pathogenesis in mice. *J. Virol.* **80,** 7976–7983 (2006).

12. Guo, Z. *et al.* NS1 protein of influenza A virus inhibits the function of intracytoplasmic pathogen sensor, RIG-I. *Am. J. Respir. Cell Mol. Biol.* **36,** 263–269 (2007).

13. Neumann, G., Hughes, M. T. & Kawaoka, Y. Influenza A virus NS2 protein mediates vRNP nuclear export through NES-independent interaction with hCRM1. *EMBO J.* **19,** 6751–6758 (2000).

14. Rossman, J. S. & Lamb, R. A. Influenza virus assembly and budding. *Virology* **411,** 229–236 (2011).

15. Chen, B. J., Takeda, M. & Lamb, R. A. Influenza virus hemagglutinin (H3 subtype) requires palmitoylation of its cytoplasmic tail for assembly: M1 proteins of two subtypes differ in their ability to support assembly. *J. Virol.* **79,** 13673–13684 (2005).

16. Rossman, J. S., Jing, X., Leser, G. P. & Lamb, R. A. The influenza virus M2 protein mediates ESCRT-independent membrane scission. *Cell* **142,** 902–913 (2010).

17. Calder, L. J., Wasilewski, S., Berriman, J. A. & Rosenthal, P. B. Structural organization of a filamentous influenza A virus. *Proc. Natl. Acad. Sci. USA* **107,** 10685–10690 (2010).

18. Seladi-Schulman, J., Steel, J. & Lowen, A. C. Spherical influenza viruses have a fitness advantage in embryonated eggs, while filament-producing strains are selected in vivo. *J. Virol.* **87,** 13343–53 (2013).

19. Kilbourne, E. D. & Murphy, J. S. Genetic studies of influenza viruses. I. Viral morphology and growth capacity as exchangeable genetic traits. Rapid in ovo adaptation of early passage asian strain isolates by combination with PR8. *J. Exp. Med.* **111,** 387–406 (1960).

20. Choppin, P. W., Murphy, J. S. & Tamm, I. Studies of two kinds of virus particles which comprise influenza A2 virus strains. III. Morphological characteristics: Independence of morphological and functional traits. *J. Exp. Med.* **112,** 945–952 (1960).

21. McCown, M. F. & Pekosz, A. Distinct domains of the influenza a virus M2 protein cytoplasmic tail mediate binding to the M1 protein and facilitate infectious virus production. *J. Virol.* **80,** 8178–8189 (2006).

22. Ruigrok, R., Baudin, F., Petit, I. & Weissenhorn, W. Role of influenza virus M1 protein in the viral budding process. *Int. Congr. Ser.* **1219,** 397–404 (2001).

23. Ali, A., Avalos, R. T., Ponimaskin, E. & Nayak, D. P. Influenza virus assembly: effect of influenza virus glycoproteins on the membrane association of M1 protein. *J. Virol.* **74,** 8709–8719 (2000).

24. Lai, J. C. *et al.* Formation of virus-like particles from human cell lines exclusively expressing Influenza neuraminidase. *J. Gen. Virol.* **91,** 2322–2330 (2010).

25. Rossman, J. S. *et al.* Influenza virus M2 ion channel protein is cecessary for filamentous virion formation. *J. Virol.* **84,** 5078–5088 (2010).

26. Bos, T. J., Davis, A. R. & Nayak, D. P. NH2-terminal hydrophobic region of influenza virus neuraminidase provides the signal function in translocation. *Proc. Natl. Acad. Sci. USA* **81,** 2327–2331 (1984).

27. Yondola, M. a *et al.* Budding capability of the influenza virus neuraminidase can be modulated by tetherin. *J. Virol.* **85,** 2480–91 (2011).

28. Barman, S. *et al.* Role of transmembrane domain and cytoplasmic tail amino acid sequences of influenza a virus neuraminidase in raft association and virus budding. *J. Virol.* **78,** 5258–5269 (2004).

29. Barman, S. & Nayak, D. P. Analysis of the transmembrane domain of influenza virus neuraminidase, a type II transmembrane glycoprotein, for apical sorting and raft association. *J. Virol.* **74,** 6538–6545 (2000).

30. Nordholm, J., da Silva, D. V, Damjanovic, J., Dou, D. & Daniels, R. Polar residues and their positional context dictate the transmembrane domain interactions of influenza A neuraminidases. *J. Biol. Chem.* **288,** 10652–60 (2013).

31. Da Silva, D. V, Nordholm, J., Madjo, U., Pfeiffer, A. & Daniels, R. Assembly of subtype 1 influenza neuraminidase is driven by both the transmembrane and head domains. *J. Biol. Chem.* **288,** 644–53 (2013).

32. Liu, H. *et al.* The ESEV PDZ-binding motif of the avian influenza A virus NS1 protein protects infected cells from apoptosis by directly targeting Scribble. *J. Virol.* **84,** 11164–74 (2010).

33. Dou, D., Silva, D. V, Nordholm, J. & Daniels, R. Type II transmembrane domain hydrophobicity dictates the co- translational dependence for inversion. (2014).

34. Iwatsuki-Horimoto, K. *et al.* The cytoplasmic tail of the influenza A virus M2 protein plays a role in viral assembly. *J. Virol.* **80,** 5233–5240 (2006).

35. Roberts, P. C., Lamb, R. A. & Compans, R. W. The M1 and M2 proteins of influenza A virus are important determinants in filamentous particle formation. *Virology* **240,** 127–137 (1998).

36. Parton, D. L., Tek, A., Baaden, M. & Sansom, M. S. P. Formation of raft-like assemblies within clusters of influenza hemagglutinin observed by MD simulations. *PLoS Comput. Biol.* **9,** e1003034 (2013).

37. Nelson, M. I. & Holmes, E. C. The evolution of epidemic influenza. *Nat. Rev. Genet.* **8,** 196–205 (2007).

Supplementary data

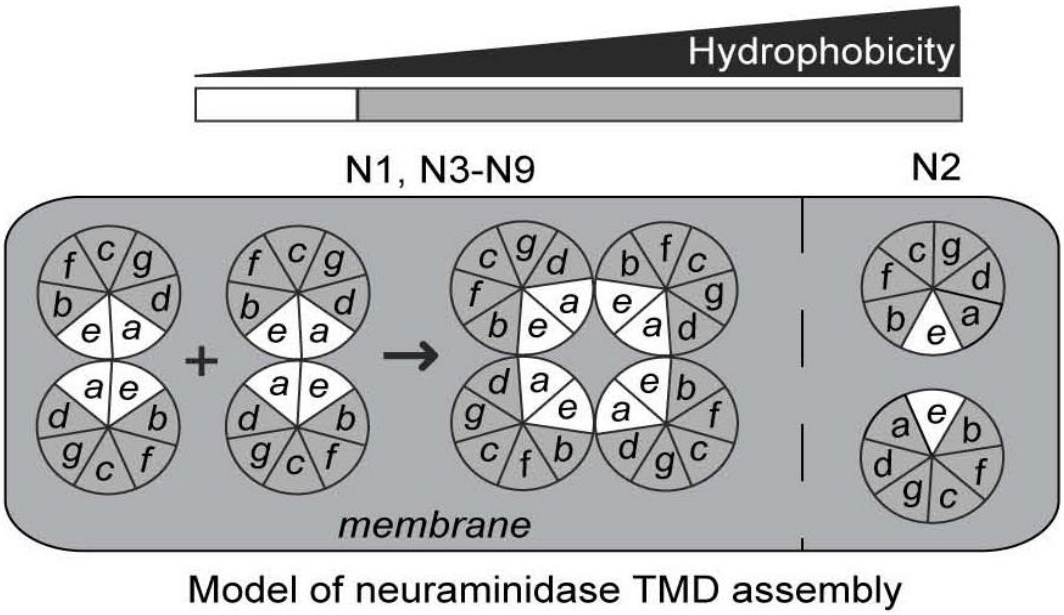

Model of neuraminidase TMD assembly

S1: Model of Transmembrane domain assembly and the alterations in hydrophobicity of TMD conferred by positioning of polar faces.

Figure S1 is showing assembly of the distinct polar face and there assembled positions amongst the varying NA subtypes. NA subtypes N1, N3 – N9 have a conserved assembled structure and positioning of polar residues and N2 subtype having differing position of polar faces within the assembled transmembrane domain (TMD). The assembled structure of TMD and structural positioning of polar faces leads to alteration in the hydrophobicity of TMD thought to alter the strength of which TMD inserts into the membrane and alter the strength of binding of NA head domain. Adapted from Nordholm et al 2013.

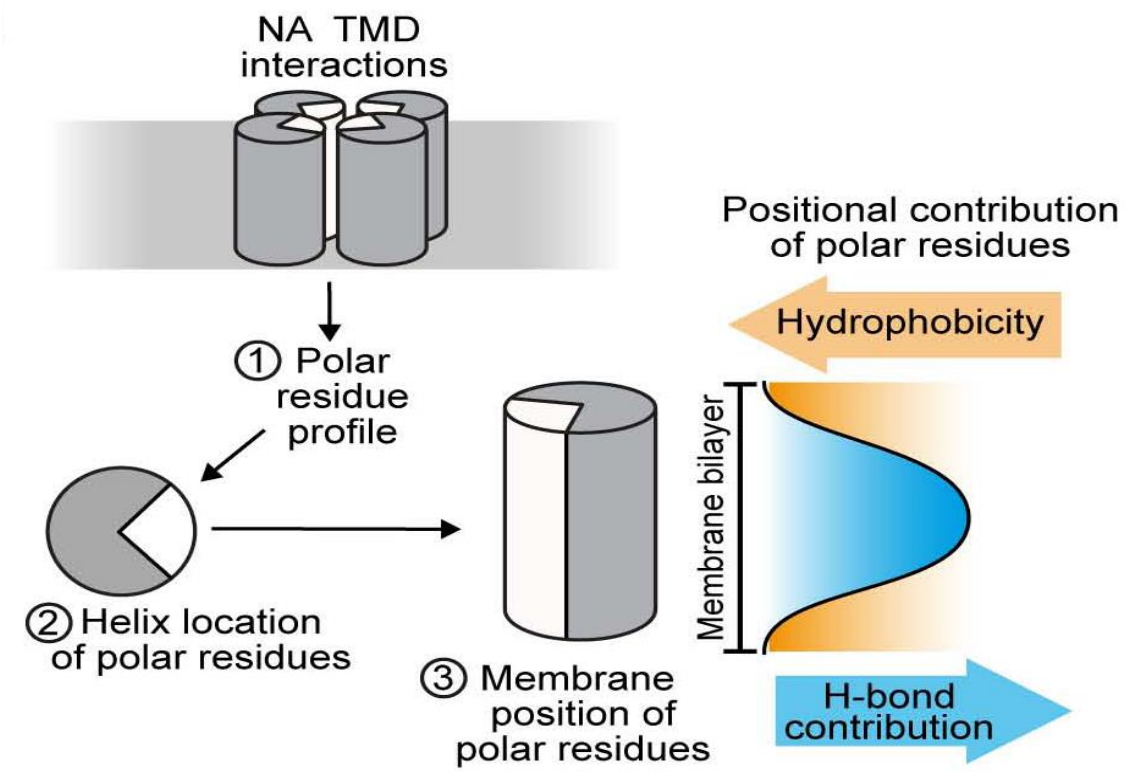

S2: Schematic of interaction between polar faces of TMD during assembly of TMD from a dimer to a tetramer and effect of residue positions.

Demonstrating current theory that the profile of polar residues present within the TMD (1) and there position within TMD assembly from a dimer to a tetramer (2), directly alter their positioning within the assembled TMD and the differential positioning of residues proportionally effects there interactions with the membrane of infected cell during its intersection during assembly of budding virion(3). Also suggested that Hydrogen bond formation and hydrophobicity of the transmembrane domain are inversely related. Figure adapted from Nordholm et al 2013.

Name	Seq. *abcdefgabcdefgabcdefgabcdefga*
$hN1_{\leq 1957}$ / WSN33	npnqkIITIGSICMVVGIISLILQIGNIISIWIs
$hN1_{\geq 1977}$	npnqkIITIGSISIAIGIISLMLQIGNIISIWAs
$hN1_{pH1N1}$	npnqkIITIGSVCMTIGMANLILQIGNIISIWIs
$hN1_{pH1N1}$ Δa	npnqkIITIGSVCMTIGMA**A**LILQIG**A**IISIWIs
$hN1_{pH1N1}$ Δe	npnqkIITIGSVCMTIGMANLIL**A**IGNIISIWIs
$hN1_{pH1N1}$ Δae	npnqkIITIGSVCMTIGMA**A**LIL**A**IG**A**IISIWIs

S3: Positioning of alanine substitutions within residues of TMD thought to be responsible for polar faces.

Showing the positioning of the alanine residue substitutions in critical residues responsible for the conserved polar faces. With sequence data representing plasmids WSN33 (WT WSN NA), hN1 pH1N1 (WSN-PN1), hN1 pH1N1 D A (WSN-PN1- \Delta-A), hN1 pH1N1 D e (WSN-PN1- \Delta-E), hN1 pH1N1 (WSN-PN1- \Delta-AE). Figure adapted from Da silva et al 2013 and provided by Robert Daniels, University of Stockholm.

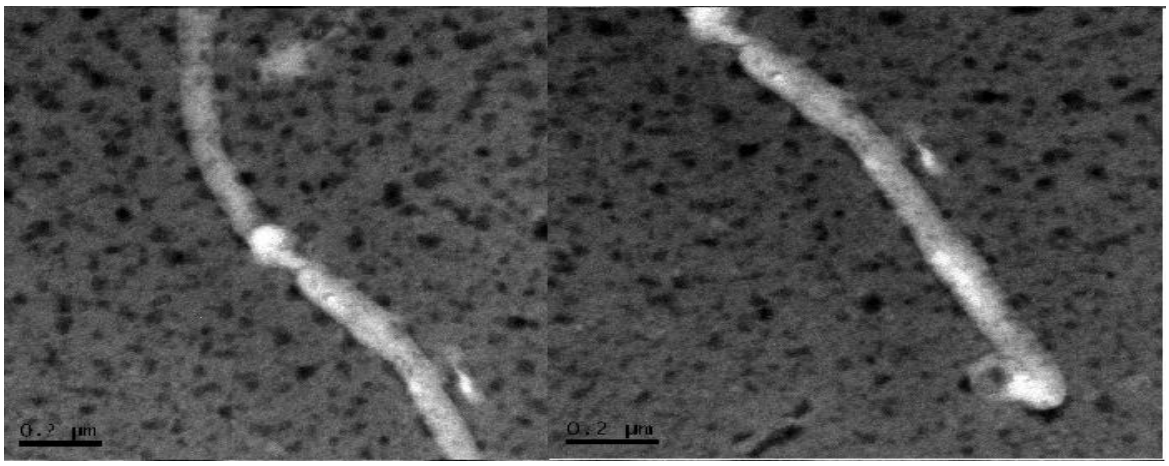

S4: Example of fragmentation and production of artefacts during concentration and imaging for TEM analysis.

Example of the production of filament like fragments caused by the concentration method required for TEM analysis. Due to pleomorphic nature of filamentous virus like particles and mature virions examination of viral and cell supernatant can be problematic in producing verifiable confirmation of filament production.

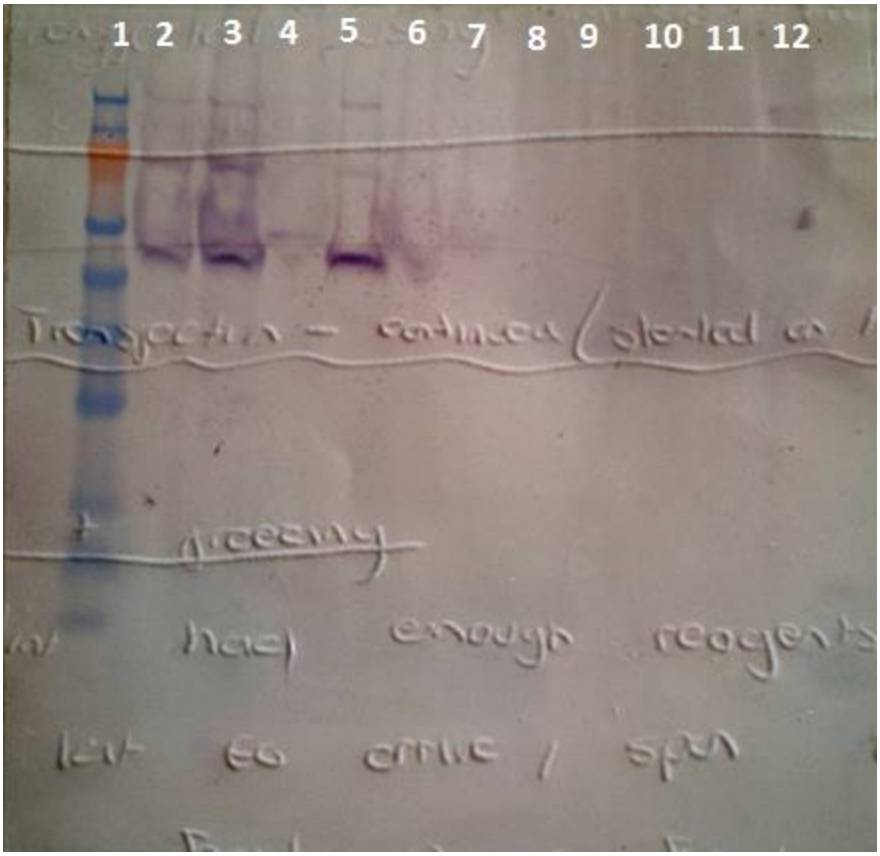

S5: Comparison of NA from transfected cell lysate and cell supernatant.

Previous repeat of HEK 293T cells transfected with NA plasmid vectors. Wells 2 -6 showing cell lysate sample and wells 8-12 showing cell supernatant samples. Lane layout as follows (1) Sea Blue 2 prestained ladder (Novex), (2) WT WSN NA, (3) WSN-PN1 NA, (4) WSN-PN1- \Delta-A NA cell lysate, (5) WSN-PN1- \Delta-E NA, (6) WSN-PN1- \Delta- AE NA, (7) Untransfected control sample of cell lysate. (8) WT WSN NA from cell supernatant, (9) WSN-PN1 NA, (10) WSN-PN1- \Delta-A NA, (11) WSN-PN1- \Delta-E NA, (12) WSN-PN1- \Delta-AE NA.

Cell lysate as shown indicates NA from transfected cells. Cell supernatant shows the same sheet like back ground staining and no expression or banding patterns indicating NA.

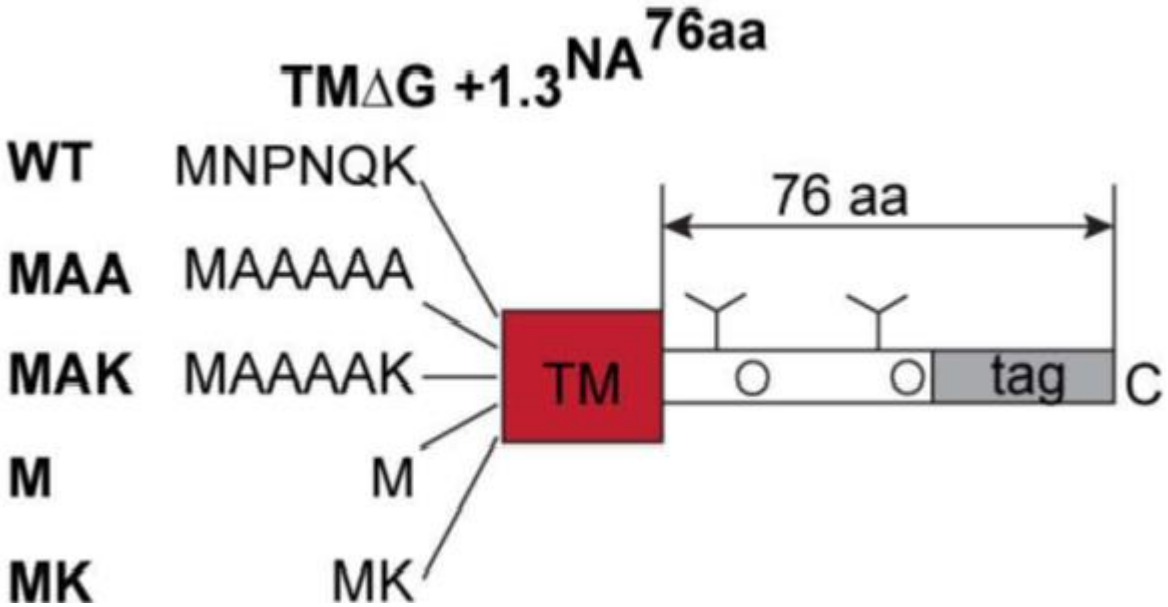

S6: Cartoon depiction of amino acid substitutions and deletions with the cytoplasmic tail and deletion of ectodomain of NA.

Figure showing deletions within the cytoplasmic tail and ectodomain region within WSN-PN1 (WSN NA with A/Swine/09 TMD) NA pcDNA3.1A plasmids in order to create the NA76 DG 1.3 pcDNA3.1A plasmid constructs used to test the ability of TMD to alter membrane curvature. Showing the various residue substitutions need to make MAA, MAK, M MK mutations within the cytoplasmic tail.